Research Article

Study on the internalization mechanism of the ZEBRA cell penetrating peptide

Roberta Marchione[1], Lavinia Liguori[2], David Laurin[1,3] and Jean-Luc Lenormand[1]

[1]TheREx, TIMC IMAG Laboratory, UMR5525, UJF/CNRS, Joseph Fourier University, 38700 La Tronche, France
[2]SyNaBi, TIMC IMAG Laboratory, UMR5525, UJF/CNRS, Joseph Fourier University, 38700 La Tronche, France
[3]Etablissement Français du Sang Rhône Alpes, La Tronche, F-38701 France

Correspondence should be addressed to Jean-Luc Lenormand; Tel: +33 476637439, E-mail: jllenormand@chu-grenoble.fr

Abstract

Cell-penetrating peptides (CPPs) represent a noninvasive method for delivering functional biomolecules into living cells. We have recently shown that the Epstein-Barr virus transcriptional factor ZEBRA contains a protein transduction domain, named Z9 or minimal domain (MD). Only few of currently identified CPPs including MD are able to rapidly cross the mammalian cell membrane without being entrapped into endosomal compartments, even when fused to cargo macromolecules. In this work, a series of MD deletion mutants has been engineered and their cellular uptake has been analyzed by confocal microscopy and FACS.

We identified a domain MD_{11} (8 amino acids shorter than MD) able to enter mammalian cells via a mainly endocytosis-independent mechanism. All the other generated truncated forms exhibited reduced cellular uptake and penetrated into cells through endocytic mechanisms. These results have highlighted the role of the MD_{11} C-terminal region as essential for efficient cellular entry and endosomal escape and open new perspectives for the use of this CPP as carrier for delivering biologically active macromolecules with therapeutic potential.

Introduction

Many therapeutic targets have been found located within cells but the effective transport of hydrophilic active molecules such as proteins or peptides across the cellular plasma membrane has represented a serious obstacle for many decades. A promising approach that seems to be the solution for overcoming the cellular barrier, has emerged with the discovery of the cell-penetrating peptides (CPPs), also referred to as protein transduction domains. Generally, CPPs are defined as relative short peptides with the ability to gain access to the cell interior and promote the intracellular delivery of conjugated cargoes (Langel 2006). Since the discovery of the first CPP from the HIV TAT protein (Frankel & Pabo 1988, Green & Loewenstein 1988), a variety of transducing peptides has been identified, including both naturally occurring domains and synthetically derived sequences. Well known examples include the penetratin peptide (Derossi *et al.* 1994), VP22 (Elliott & O'Hare 1997), pVEC (Elmquist *et al.* 2001), polyarginine (Mitchell *et al.* 2000), Transportan (Pooga *et al.* 1998), etc. The common feature of CPPs is their typically high content in basic arginine and lysine residues, leading to a positive net charge of the peptides, which is considered to be crucial for initial membrane interaction through binding to negatively charged phospholipids and glycosaminoglycans (Ziegler 2008). The number of applications using CPPs is increasing, and so far more than 300 studies from in vitro to in vivo have been reported (Heitz *et al.* 2009). Indeed, the interest for CPPs is mainly due to their low cytotoxicity and to the fact that there is no limitation for the type of cargo. CPPs have been used to improve delivery of cargoes that vary greatly in size and nature, including small molecules, oligonucleotides, plasmid DNA, peptides, proteins, nanoparticles, virus and lipid-based formulations (Zorko & Langel 2005). Despite the similarities among CPPs, the translocation mechanisms may vary considerably. The two main pathways suggested for cellular uptake are direct penetration and endocytosis (Madani 2011). However, the impact of these two mechanisms on the biological function of the transported cargo is different. Contrary to direct penetration, during endocytosis, the cargo can be entrapped and consecutively partially degraded into endosomal compartments, thus leading to the loss of its activity. This aspect represents the main limitation

towards the therapeutic use of CPPs as delivery systems for biologically active drugs. When conjugated to cargo molecules, the cellular uptake of most widely used CPPs such as penetratin, TAT, pVEC and transportan is shown to proceed through an endocytic pathway (Eiriksdottir *et al.* 2010, Lundin *et al.* 2008, Saalik *et al.* 2004). In a previous study, we identified a novel cell-penetrating peptide able to cross the cell membranes in an endocytosis-independent mechanism even when fused to cargoes, as shown with eGFP and β-galactosidase reporter proteins (Rothe *et al.* 2010). This CPP derives from the Epstein-Barr virus (EBV) ZEBRA transcription factor. A reductionist study of full-length ZEBRA protein has allowed us to identify the amino acid region (named as Minimal Domain, MD) implicated in cellular uptake (Rothe *et al.* 2010). The region required for internalization spans residues 170-220 from the ZEBRA protein and contains two contiguous domains: a positively charged domain (DNA-binding domain, DBD) and a hydrophobic leucin-rich domain (dimerization domain, DIM). The DBD is believed to mediate cell surface binding of the MD to the negatively charged heparan sulfate proteoglycans while the DIM domain facilitates translocation through the lipid bilayer by hydrophobic interactions (Rothe *et al.* 2010).

In the present study, we aimed at reducing the size and the hydrophobicity of the transduction domain and at describing the amino acid sequence required for its cellular uptake. We produced MD truncations in fusion to the eGFP reporter protein and evaluated the ability of these constructions to translocate through the membrane of HeLa cells. We identified a MD shorter peptide (MD_{11}) able to enter mammalian cells with high efficiency by an endocytosis-independent mechanism. Further trimming of the DIM domain from the MD_{11} peptide led to a decrease in the translocation efficiency and to an alteration of the uptake mechanism. The results presented here reveal the role of the whole DIM domain as necessary for endocytosis-independent cell internalization. This import mechanism is an attractive requisite for developing MD_{11}-mediated uptake of macromolecules in therapeutic applications and strengthens this delivery system compared to most others.

Materials and Methods

Cloning, expression and purification of the MD_x-eGFP fusion proteins

The cloning, the expression and the purification of the free eGFP and the recombinant fusion proteins MD_x-eGFP were performed as described in Rothe and Lenormand (2008). Briefly, the DNA fragments encoding for the MD deletion mutants were generated by PCR and ligated upstream of the 5'-end of eGFP gene into pET15b expression plasmid, bearing a His_6-tag sequence. The generated MD truncations are schematically depicted in Figure 1A. The fusion recombinant proteins were produced in *E. coli* BL21 (DE3) cells by inducing the expression with 0.5mM Isopropyl β-D-1-thiogalactopyranoside (IPTG) at OD_{600nm} of 0.8 for 18h at 16°C. In order to recover the proteins of interest, the bacterial cultures were centrifuged at 5000g for 15 min and the cell pellets were sonicated in 20mM Tris/HCl pH 7.4, 500mM NaCl, 10% glycerol, 2mM DTT, 10mM imidazole (5mL per gram wet pellet) supplemented with a complete protease inhibitor cocktail (Roche). As all the MD_x-eGFP were produced with a hexahistidine tag, the soluble fractions were purified onto nickel sepharose HisGraviTrap columns (GE Healthcare) by gravity-flow and eluted in the same buffer by a stepwise increase (at 100, 175, 250 and 500mM) of imidazole content. MD_x-eGFP proteins were separated onto a 15% SDS-polyacrylamide gel electrophoresis and analyzed by Coomassie blue staining or by Western-blotting using an anti-His tag antibody HRP-coupled (Sigma, 1:10000 dilution). Prior to their use for cellular uptake experiments, purified eGFP and MD_x-eGFP proteins were dialyzed against PBS and 25mM HEPES/KOH pH7.0, 150mM NaCl and 10% glycerol respectively using a MWCO 8000 SpectraPor^{TM} dialysis tubing (Spectrum Laboratories). The yield of the purified His-tagged proteins was quantified by BCA Protein Assay Kit according to the manufacturer's instructions (Pierce).

Helical wheel projections of the peptides were generated using online program available at http://rzlab.ucr.edu/scripts. Primary sequence analysis was performed using EMBOSS bioinformatics programs and the GRAVY index was calculated using ProtParam tool at ExPASy Proteomics Server.

Cell culture
HeLa cells were maintained in DMEM (PAA, GE Healthcare) supplemented with 10% heat-inactivated fetal bovine serum (PAA, GE Healthcare), 100 units/mL penicillin and 50μg/mL streptomycin (Gibco). Cells were cultured at 37°C in a humidified 5% CO2 atmosphere incubator.

Confocal microscopy
HeLa cells (5×10^4 cells/well) were seeded onto an 8-well Lab-Tek^{TM} chambered coverglass (Nunc) in complete cell culture media 24h before treatment. After removal of the medium, the cell layers were rinsed twice with DPBS and subsequently exposed at 37°C for 4 hours to 0.3μM of recombinant proteins in fresh
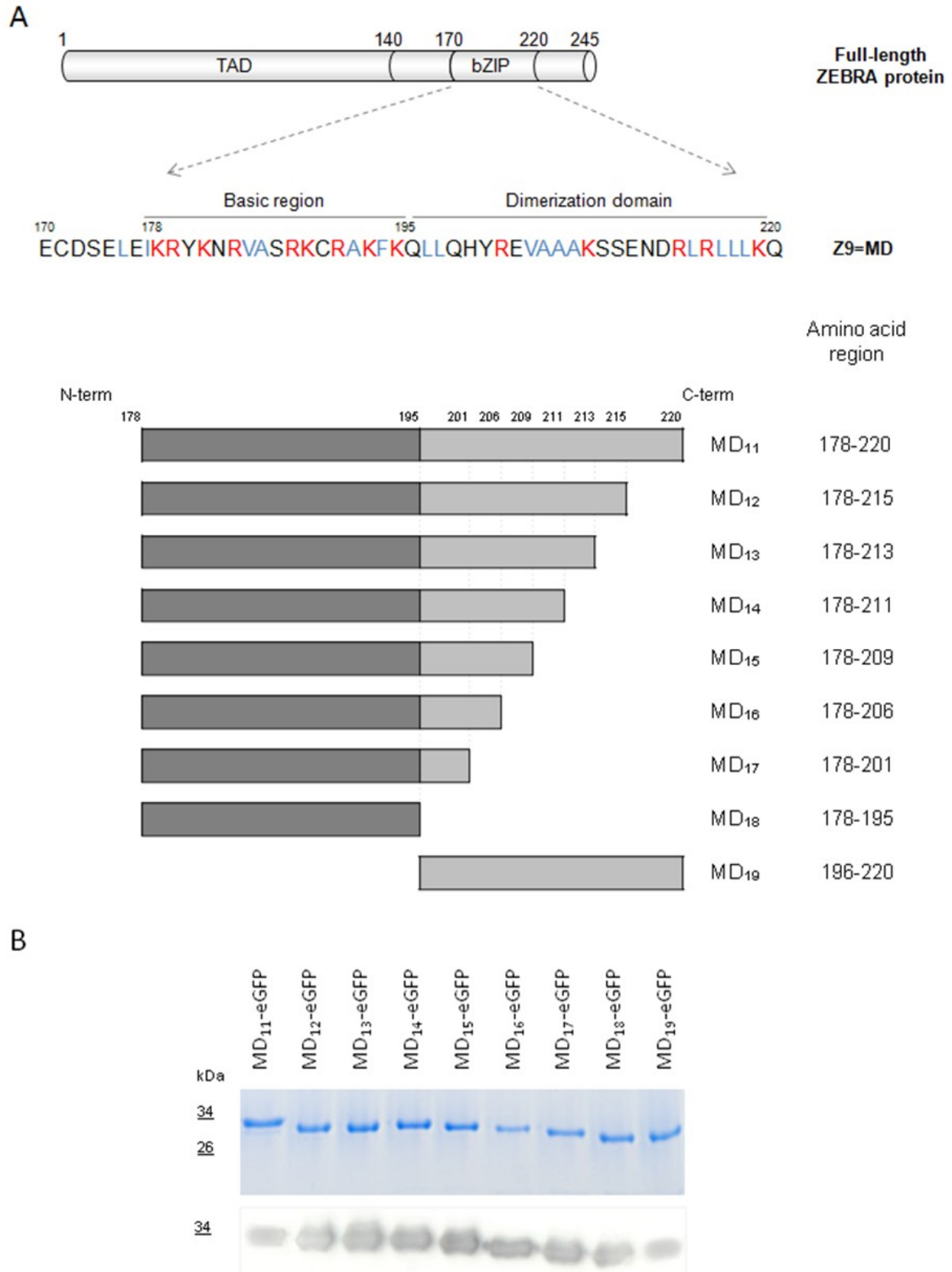
Figure 1. A) Amino-acid sequence of ZEBRA MD cell-penetrating peptide (aa 170-220) and scheme of the deletion mutants. Amino acids are designated with one-letter code and numbered according to the full-length ZEBRA protein sequence. Basic amino acids are shown in red, whereas hydrophobic amino acids in blue. B) Recombinant fusion proteins, containing each peptide fused to the N-term of eGFP, were separated on a 15% SDS-polyacrylamide gel and visualized by Coomassie Blue staining and detected by Western blotting using anti-His antibody.

serum-free medium. Thereafter, the incubation solutions were removed and the cells were washed three times with DPBS. Living cell preparations were observed with a LSM 710 confocal scanning laser microscope (Carl Zeiss, Jena, Germany), using a 63×, NA 1.2, C-apochromat water-immersion objective (Carl Zeiss). The experiment was carried out at 488nm excitation and fluorescence was collected with a 510-560 nm filter. 16 successive optical slices were captured along the cell z axis, with a step of 1μm. For localization study, cells were also fixed for 15 minutes in 4% paraformaldehyde at room temperature and then stained with 10μM Nile Red. The images were acquired with 488nm for eGFP and 633nm for Nile Red excitation and fluorescence was collected between 502 – 541 and 580 – 668nm filters respectively.

Cellular uptake assays
For transduction experiments, 1.5×10^5 HeLa cells/well were cultured on 12-well plates until 70% of confluence. Cells were washed twice with DPBS and incubated with 0.3μM of recombinant proteins in fresh serum-free culture medium for 4 hours at 37°C. After incubation, cells were trypsinized with 0.5% trypsin/EDTA solution (PAA, GE Healthcare) for 10 min at 37°C to remove the extracellular bound proteins. The trypsin was then neutralized by adding complete medium and the cells were washed twice with DPBS.

For endocytic inhibition experiments, cells were first pre-incubated for 30 minutes with different endocytic inhibitors at the following concentrations: 50μg/mL nystatin, 100nM wortmannin and 5mM methyl-β-cyclo-dextrin (Sigma). After pre-incubations with the endocytic inhibitors, the recombinant proteins were added to cell cultures in the presence of drugs and treated as indicated above.

Cell-associated fluorescence was detected using a FACS Canto II BD Biosciences flow cytometer. We used a 488nm laser for excitation and 530/30 bandpass filters for emission. The results are reported as the mean fluorescence intensity from living cells gate of 30000 events recorded and analyzed with the FACSDiva software.

Differences between samples and treatments were evaluated by variance analysis (two-tails, paired values) followed by the least-significant difference test. A difference was considered to be statistically significant with $p < 0.05$.

Preparation and observation of lipid vesicles
Giant unilamellar vesicles (GUVs) were created by sucrose hydration method (Akashi *et al.* 1996). Three different lipid compositions were used in order to obtain fluid (100% PC), rigid (SM:Chol 50:50 % molar ratio) and semi-fluid (PC:SM:Chol 33:33:33 % molar ratio) GUVs. 50μg of lipid mixtures in chloroform were deposited in an 8-well Lab-Tek™ chambered coverglasses and dried under nitrogen. The dried film was hydrated overnight at 4°C with 25mM HEPES/KOH pH7.4, 250mM sucrose. After re-hydration, 1μg of MD-eGFP was added to GUV solution. The lipid component was labeled with Nile Red dye (10μM), and CSLM images were acquired as described above.

Results

Design and expression of MD analogs
The ZEBRA MD protein transduction domain (amino acids 170-220) consists of 14 basic residues (Lys and Arg) and 15 hydrophobic residues, mainly located at the C-terminal dimerization domain (Figure 1A) (Rothe & Lenormand 2010). To better understand the specific contribution of the different amino acids in the internalization process, we designed a series of iterative MD truncation mutants. An initial deletion was realized by removing the first eight amino acid residues located upstream of the basic region at the N-terminus of the MD, resulting in a sequence named as MD_{11} (Figure 1A). In transduction experiments on HeLa cells, recombinant proteins containing MD_{11} fused to the fluorescent reporter protein eGFP were able to penetrate with the same efficiency as MD (Rothe & Lenormand, unpublished data). Thus, we decided to further optimize this CPP (MD_{11}) by reducing its size and increasing its hydrophilicity. We engineered six truncations by removing from a minimum of five to a maximum of nineteen amino acids from the hydrophobic C-terminus (Figure 1A). In addition, we produced two more truncations containing either only the basic (MD_{18}) or the hydrophobic (MD_{19}) region. We then expressed each peptide fused to the N-terminal end of eGFP. The his-tagged recombinant fusion proteins were produced using an E. coli expression system and purified by nickel affinity chromatography. The purity of the MD_x-eGFP proteins was analyzed by Coomassie blue staining and by western-blotting using an anti-his antibody (Figure 1B). Recombinant proteins were pure at around 85%.

A crystallographic study has revealed that the DNA-bound ZEBRA protein (residues 175-245) is an extended bZIP helix (Petosa *et al.* 2006). With the use of the helical wheel projections, the sequences of the MD truncations were examined (Figure 2). The wheels for all deletions have both a polar and a hydrophobic character. In each helix, there are two spatially organized regions of polar residues interrupted by a few hydrophobic residues. The exact content in polar and non-polar residues for each truncation is summarized in
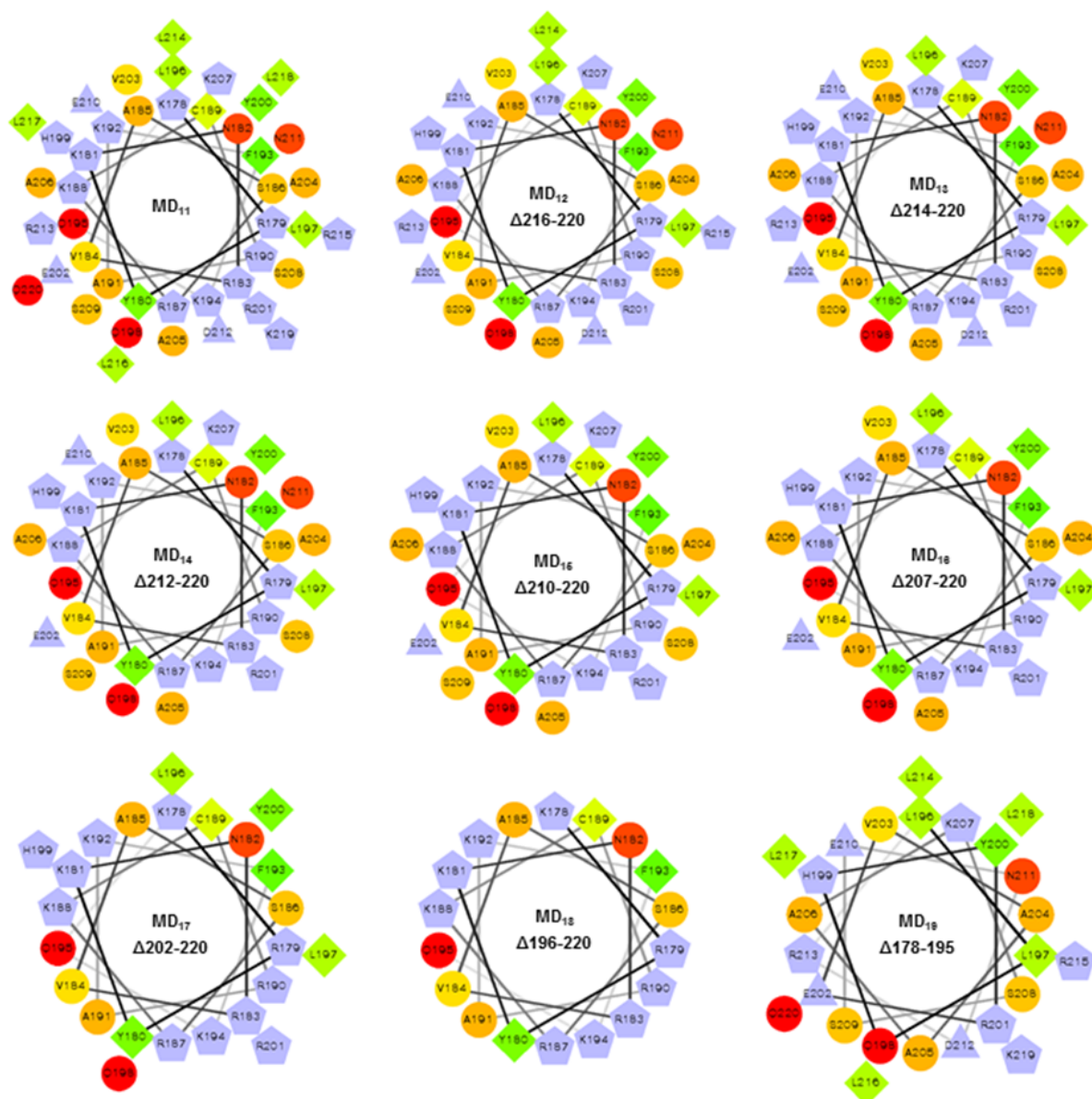
Table 1

Peptide	Number of residues	Net charge at pH 7	Positive charges K, R, H	Negative charges D, E	Aromatic residues Y, F	Polar residues (without net charge) N, Q, S	Non polar residues A, C, F, I, L, V, Y	Grand average of hydropathicity (GRAVY)
MD11	43	11,5	15	3	3	8	17	-1.151
MD12	38	10,5	14	3	3	7	14	-1.408
MD13	36	9,5	13	3	3	7	13	-1.467
MD14	34	9,5	12	2	3	7	13	-1.318
MD15	32	10,5	12	1	3	6	13	-1.181
MD16	29	9,5	11	1	3	4	13	-1.114
MD17	24	10,5	11	0	3	4	9	-1.600
MD18	18	9	9	0	2	3	6	-1.861
MD19	25	2,5	6	3	1	5	11	-0.640

Figure 2. Helical wheels projections of MD$_{11}$ and its truncated analogs. The projections were realized using the online program available at http://rzlab.ucr.edu/scripts. The hydrophilic residues are presented as circles, hydrophobic residues as diamonds, potentially negatively charged as triangles, and potentially positively charged as pentagons. The most hydrophobic residues are presented in green, and the amount of green is decreasing proportionally to the hydrophobicity (with zero hydrophobicity coded as yellow). Hydrophilic residues are coded red, and the amount of red is decreasing proportionally to the hydrophilicity. The charged residues are light blue. The peptide length, the amino acid composition, and the GRAVY index of each peptide are indicated in the Table 1. The parameters were calculated using EMBOSS and ExPASy bioinformatics programs.
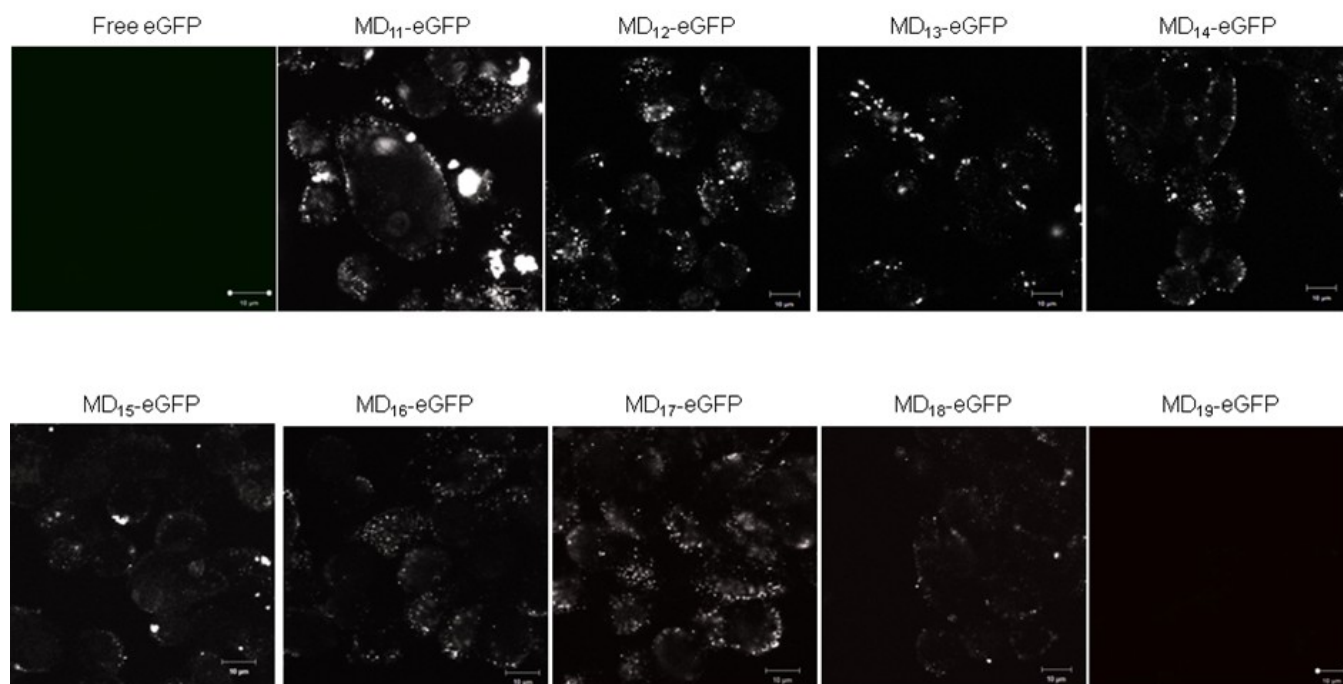
Figure 3. Confocal laser scanning microscopy images of living HeLa cells incubated for 4 hours with 0.3μM of free eGFP and MD_x-eGFP fusion proteins. 16 successive optical slices were captured along the cellular z-axis with a step of 1μm. The presented images correspond to the middle plan of cellular z-axis sectioning.

the Table 1. In all cases, except for MD_{19}, the peptides are net positively charged. The shortening and deletion of the DIM domain affect both charge and hydrophobicity contributions: the non-polar and negative amino acid content is reduced and the hydrophilicity (negative GRAVY value, (Kyte & Doolittle 1982)) of the peptides is increased.

Confocal microscopy
The transduction ability of MD deletions was investigated by confocal microscopy on living HeLa cells after 4 hours treatment with 0.3μM of each recombinant protein according to results reported in Rothe *et al.* (2010). The cellular uptake and the intracellular distribution of the recombinant proteins were checked by direct visualization of the intracellular eGFP fluorescence. As expected, no fluorescence signal was detected on HeLa cells incubated with free eGFP (Figure 3). Except for MD_{19}, Z-stack analysis of treated cells confirmed that MD_{11} and most of its analogs maintained the cell penetrating ability (Figure 3). The degree of intracellular fluorescence accumulation varied between the different MD_x constructions (Figure 3). To better delineate cell contours and evaluate the interaction of the recombinant cell-penetrating proteins with membranes, cells were also fixed and the membrane lipids stained with the fluorescent dye Nile Red (Figure 4). Overlapping green and red images resulted in yellow signals demonstrating the co-localization of

MD_{11}, MD_{14}-MD_{17} eGFP fusion proteins with membrane lipids (Figure 4).

Cellular uptake assays
To quantify the cellular uptake of MD_{11} and its truncated forms, FACS analysis was performed after a four-hour incubation of living HeLa cells with 0.3μM of each fusion protein. The extra-bound fluorescent proteins were removed by trypsin digestion. All peptides were found to penetrate into cells, but the new derived MD_{11} peptides differed remarkably in efficiency of penetration (Figure 5A). No improvement of uptake was observed when the number of MD_{11} amino acid residues was further reduced. Indeed, the maximum efficiency of internalization was observed in HeLa cells incubated with MD_{11}-eGFP.

To evaluate the internalization mechanism of MD_{11} and its truncations, we measured their uptake efficiency in living cells in presence of three endocytosis inhibitors. Nystatin was employed to inhibit the caveolae-mediated endocytosis, wortmannin to inhibit macropinocytosis, and MβCD to disrupt the import through lipid rafts. The presence of nystatin and wortmannin did not interfere with MD_{11}-eGFP internalization (Figure 5B), indicating no participation of the receptor-mediated endocytosis in its uptake process. Incubation with MβCD caused a 30% decreased uptake of MD_{11}-eGFP. Thus, the endocytotic pathway contributed only partially to the MD_{11}-eGFP cellular uptake

under the applied conditions but did not account for the majority of the internalized fusion protein. In contrast, a strong decrease in the uptake of MD_{12-19} truncations was observed when the three analyzed endocytosis pathways were inhibited, indicating that the main internalization routes of these peptides were both receptor- and lipid raft- mediated endocytosis. Thus, MD_{11} is the shortest CPP derived from the EBV ZEBRA transcription factor with the highest internalization efficiency through a mainly endocytosis-independent mechanism.

Confocal imaging of MD_{11} peptide-lipid interaction
To further examine the interactions of MD_{11} with lipids, we incubated the fusion protein MD_{11}-eGFP with lipid vesicles of different composition and rigidity. Kinetics of protein-lipid interactions, membrane rigidity and changes in membrane morphology can be easily evaluated by microscopy imaging because of the giant vesicle's size. Fluid vesicles were prepared using phosphatidylcholine (PC 100%), rigid and semi-fluid vesicles were obtained by mixing sphingomyelin and cholesterol (SM, Chol 50:50% molar ratio) and PC,

SM, Chol (33:33:33% molar ratio) respectively. The Nile Red dye (2μg/ml) was used to stain the lipids. MD_{11}-eGFP fusion protein was incubated with vesicles for 1, 2.5, 3.5, 4.5 and 24 hours at 37°C, and the protein-lipid interaction was monitored by confocal laser scanning microscopy. All the vesicles were homogenously stained with the red dye. We noticed a time-dependent accumulation of green fluorescent signal (eGFP) surrounding the vesicle membranes in all the tested conditions. By overlapping the two fluorescent signals (red from the Nile red and green from the eGFP), it is possible to evaluate the interaction of peptide-lipid that results in a yellow staining of the vesicle membranes. After 3.5 h incubation, three different patterns of co-localization were observed (Figure 6, "merge" panel). A strong co-localization of MD_{11} peptide was recorded on semi-fluid and rigid vesicles containing both SM and Chol (Figure 6B and 6C). Any interaction was observed between MD_{11} and PC fluid vesicle membranes (Figure 6A), even after 24 hours (data not shown). Curiously, a heterogeneous interaction of MD_{11} in restricted clusters of semi-fluid vesi-
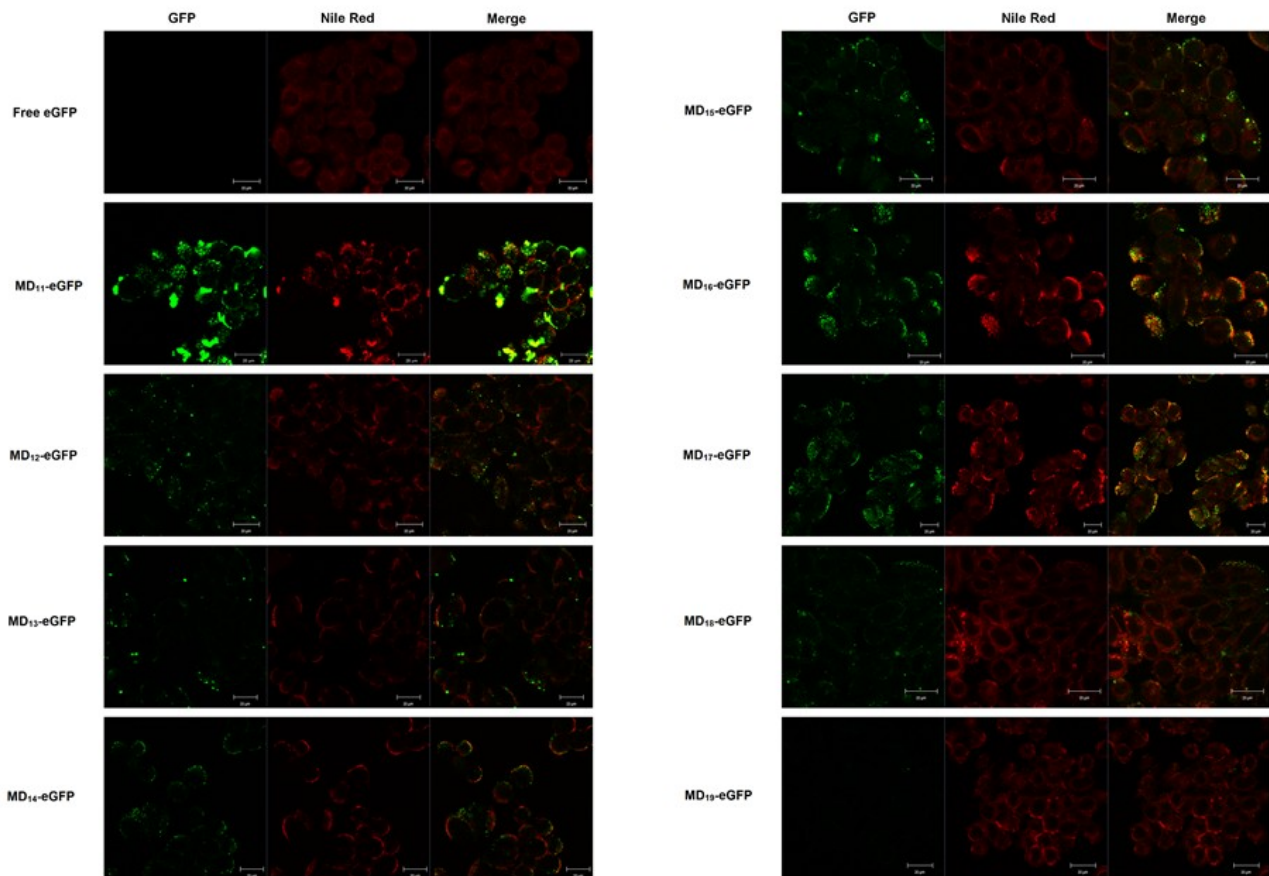

Figure 4. Intracellular localization of MD_x-eGFP in HeLa cells. Confocal microscopy images of fixed HeLa cells after a 4-hour incubation with 0.3μM of free eGFP and MD_x-eGFP fusion proteins. MD_x-eGFP signals are shown in green and the cellular lipid component in red. The showed images correspond to the central plane of cellular z-axis sectioning.
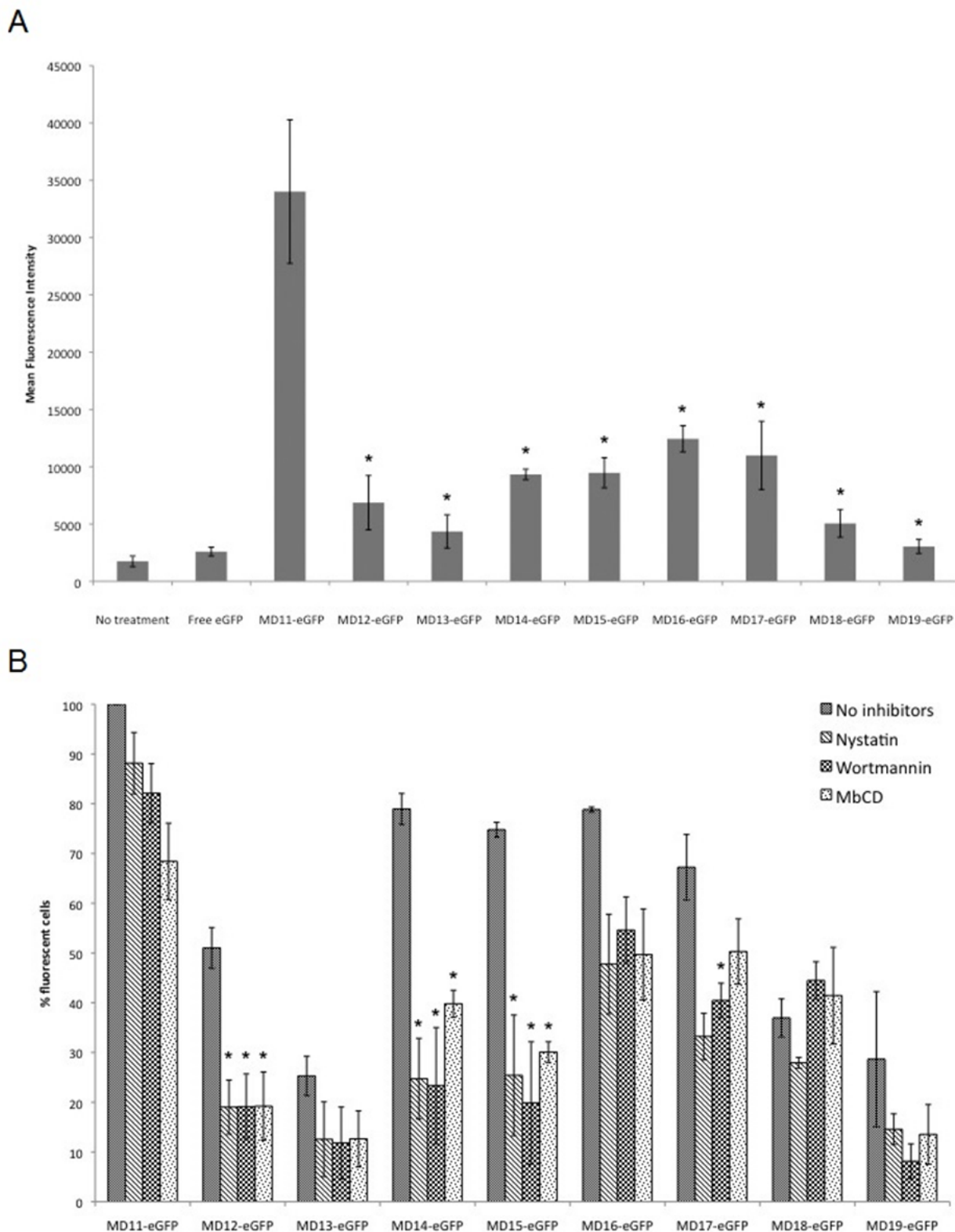
Figure 5 FACS cellular uptake of MD_{11} and its truncated analogs. A) HeLa cells were incubated with 0.3µM of different peptides fused to eGFP for 4h at 37°C. The data are expressed as mean fluorescence intensity (MFI) of eGFP positive cells and the values indicated are the mean±s.d. of four independent experiments. *$p < 0.05$ MD_{11}-eGFP versus each $MD_{(12-19)}$-eGFP

B) Uptake of MD_{11} and its truncated analogs in presence of endocytosis inhibitors. HeLa cells were pre-treated with 50µg/mL nystatin, 0.1µM wortmannin or 5mM MβCD for 30min at 37°C. 0.3µM of recombinant proteins were incubated with cells for 4h at 37°C. The data are expressed as % of eGFP positive cells and the values indicated are the mean±s.d. of two independent experiments. All fluorescence values have been normalized assuming as 100% the number of fluorescent cells incubated with the MD_{11}-eGFP without inhibitors. *$p < 0.05$, $MD_{(11-19)}$-eGFP without inhibitors versus the same MD in presence of different inhibitors.
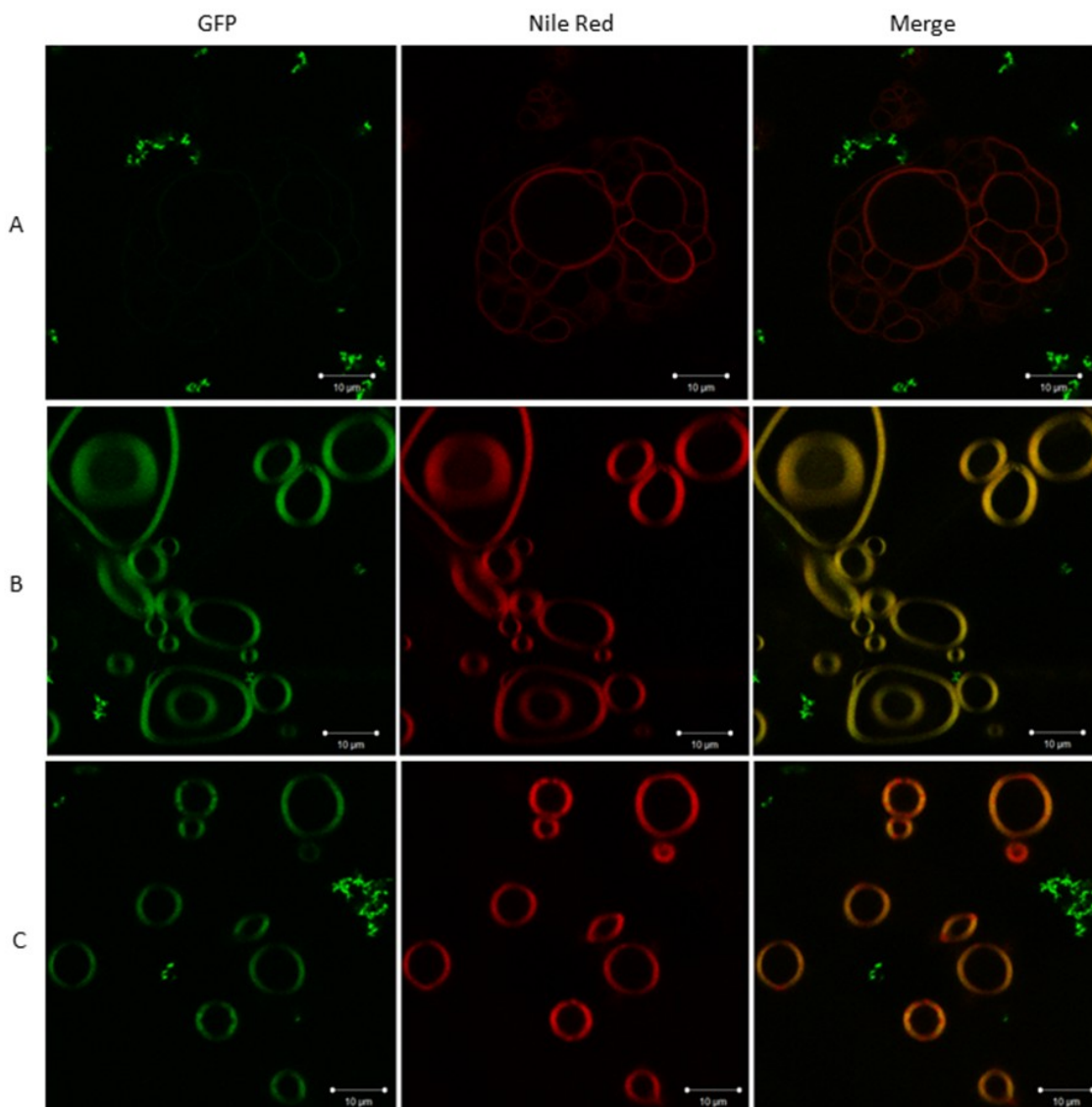
Figure 6. Confocal imaging of $MD_{11}eGFP$-GUV interaction after 3.5h treatment. MD_{11}-eGFP was incubated with A) fluid (100% PC), B) rigid (SM:Chol 50:50 % molar ratio) and C) semifluid (PC:SM:Chol 33:33:33% molar ratio) GUVs. MD_{11}-eGFP signal is shown in green and the lipids in red. The co-localization of the peptide on lipid membranes is shown in the merge panel.

cles was observed after one hour incubation (data not shown).

Discussion

Increasing efforts are currently being made for developing CPPs as delivery systems for therapeutic macromolecules. In this context, the identification of their cellular uptake mechanisms is essential for optimization of appropriate strategies. The majority of CPPs is internalized via endocytosis when coupled to cargo molecules (Eiriksdottir *et al.* 2010, Lundin *et al.* 2008, Saalik *et al.* 2004). This aspect represents a great limit because payload molecules can be entrapped and degraded into endosomal vesicles, with the consequent loss of their biological activity. Due to a potential degradation of the CPP-coupled molecule, this internalization mechanism does not represent a method of choice for the cellular transfer of therapeutic cargoes. There-

fore, identification of new CPPs endowed with direct translocation mechanism is necessary. Recent protein complementation assays have been developed to confirm the cellular uptake of cargoes mediated by CPPs and the endosomal escape of biologically active molecules (Milech *et al.* 2015).

We have recently shown that EBV ZEBRA protein contains a 51 amino acid- sequence (residues 170-220, MD) able to transduce across mammalian cellular membranes by an endocytosis-independent mechanism (Rothe *et al.* 2010). MD peptide contains two regions: the basic DBD and the adjacent leucin-rich DIM domain. Previous results indicated that the presence of both domains could be essential for MD cellular uptake (Rothe *et al.* 2010). Furthermore, enzymatic activity has been detected even in cells transduced with MD fused to high-molecular weight protein, such as β-galactosidase (116kDa) (Rothe *et al.* 2010). This evidence prompts us toward further inves-

tigations to explore the employment of MD as carrier of therapeutic macromolecules. The identification of a shorter MD peptide able to enter cells by an endocytosis-independent mechanism is suitable for developing efficient drug delivery strategies. For this purpose, different MD truncations have been designed with the aim to reduce the carrier size and preserve its mechanism of internalization. The direct translocation of hydrophilic cargoes to intracellular compartments represents a great advantage for therapeutic applications as they can be directly delivered into cells in an active state without being entrapped and degraded in endosomes/lysosomes. As the presence of a cargo may influence the internalization process, MD peptides were fused to the eGFP reporter protein and their cellular uptake was investigated by confocal microscopy and FACS analysis.

Starting from an eight amino acid shorter peptide (MD_{11}), six different peptides were produced by reducing the C-terminal end, and two were generated by isolation of DBD (MD_{18}) and the DIM (MD_{19}) domains. All DIM-deleted peptides possess protein transduction properties, even though the highest efficiency has been observed in cells incubated with the original MD_{11}-eGFP protein. Unlike the DIM domain (MD_{19}), the peptide containing only DBD domain (MD_{18}) can pass through the cell membranes, indicating that the cationic charges may play an important role in the uptake mechanism. To quantify the peptide cellular uptake, FACS analysis was performed. In agreement with qualitative data obtained by confocal microscopy, size reduction of the DIM domain induces a decrease in translocation efficiency. Fluorescence values normalized to the highest recorded signal of MD_{11} show a decrease of about 70% for all DIM-deleted peptides and the absence of internalization for MD_{19}-eGFP (DIM domain only).

We can first explain these results considering that the decrease in length of DIM domain could entail structural modifications of MD_{11} helix affecting its penetrating activity. Secondly, as shown for TAT peptide (Hoyer *et al.* 2012), MD_{11} could penetrate into cells in dimer form and the reduction of the DIM sequence might prevent this process inducing a decrease in the internalization efficiency.

Curiously, the loss in uptake is not directly linked to the number of removed amino acids. In fact, we observe that the deletion of five or seven residues (MD_{12} and MD_{13} respectively) induces a lower cytoplasmic accumulation than the uptake mediated by MD_{16} and MD_{17}. The analysis of the primary sequences shows that, similarly to MD_{11}, both MD_{16} and MD_{17} possess a repeated motif at C-terminal end. This motif is composed of two or three successive hydro-

phobic residues (Leu or Ala) followed by a basic (Lys) and/or a polar (Gln or Ser) residue. Probably, the presence of this motif is involved in the interaction with hydrophobic membrane lipids and may regulate the cellular uptake. These pieces of evidence highlight that the length of the MD helix and its polar character play a key role in the internalization process.

To check the impact of chain length reduction on internalization mechanism, we investigated the uptake of MD_{11} and its derived peptides in presence of endocytosis inhibitors. Inhibition of caveolae-mediated endocytosis and macropinocytosis does not affect MD_{11}-eGFP uptake, whereas the internalization of all MD_{11} deleted forms is strongly impaired. This loss of endocytosis-independent mechanism is also suggested by the presence of vesicles-like structures in cytoplasm of HeLa target cells incubated with MD_{16} and MD_{17} fusion proteins (Figure 4). These results demonstrate that (i) the MD_{11}-mediated cellular import is neither based on caveolae-mediated endocytosis nor on macropinocytosis and (ii) the deletion of DIM domain induces a switch from a non-endocytic to an endocytic pathway. Future optimizations of MD_{11}-derived CPPs need to take into account that all the residues of the DIM domain are required to guarantee the endocytosis-independent internalization.

To elucidate the roles of lipids in MD_{11}-membrane interactions, we used fluid (PC), rigid (SM, Chol) and semi-fluid (PC, SM, Chol) vesicles. We show that MD_{11} peptide strongly interacts with sphingomyelin and cholesterol, but not with phosphatidylcoline. These evidences well correlate with FACS data on living cells indicating that the depletion of cholesterol by MβCD treatment can have an impact on the MD_{11} entry. Since SM and cholesterol are both involved in lipid raft formation (Simons *et al.* 1997), we suggest that MD_{11} may interact with lipid-raft membrane domains during internalization. However, any significant accumulation in vesicles' lumen has been detected after MD_{11}-eGFP incubation. Our findings are in agreement with results on other CPPs such as R12-HA, Pep-1 and MPG, that are known to enter cells in endocytic-independent manner, and are not able to translocate and accumulate in artificial vesicles (Deshayes *et al.* 2004, Henriques *et al.* 2004, Hirose *et al.* 2012). These studies have established that direct translocation is strongly dependent on the presence of a negative membrane potential, and is modulated by the lipid composition, the membrane curvature and the local peptide concentration (Henriques *et al.* 2004, Hirose *et al.* 2012, Terrone *et al.* 2006). Furthermore, artificial membranes represent a simplified system compared to biological membrane, and a combination

of different methods is necessary to fully clarify the MD$_{11}$ entry mechanism.

Recent studies have reinforced the notion that a characteristic for direct translocation of CPPs is the presence of a hydrophobic moiety and have proved that this process occurs at specific locations of the plasma membrane (Hirose *et al.* 2012, Palm-Apergi *et al.* 2012). The attachment of a hydrophobic peptide tag deriving from human influenza hemagglutinin greatly accelerates the direct penetration of dodeca-arginine (R12) cationic peptide (Hirose *et al.* 2012). The hydrophobicity of the coupled peptide stimulates dynamic morphological alterations in the plasma membrane, which allow the permeation through the lipid bilayer (Hirose *et al.* 2012). Since the DIM domain of the MD$_{11}$ is hydrophobic, we believe that it acts in a similar way and can stimulate the internalization in an endocytosis-independent manner. It was previously demonstrated that the amino acid Leu217 located into the DIM domain was required for the homodimerization of ZEBRA and may avoid heterodimirezation of ZEBRA with other bZIP proteins (Petosa *et al.* 2006). The decrease of cellular uptake with our deletion mutant MD$_{12}$-eGFP indicates that the removal of Leu217 amino acids may impact first, on the dimerization of ZEBRA and then, on the transduction capacities of the mutant. Other CPPs such as Antennapedia (Antp) or 30Kc19 have a dimerization propensity at the plasma membrane for stimulating the internalization process (Derossi 1994, Park *et al.* 2014). Like these CPPs, the hydrophobic environment of the DIM domain is important for the cellular uptake. According to these pieces of evidence, we believe that the charged DBD domain is involved in the initial interaction with the bilayer while the hydrophobic domain is crucial for its insertion.

In conclusion, with the present study we demonstrate that the MD$_{11}$ C-terminal DIM domain contributes to the internalization but doesn't act as a driving force in this process and that it regulates the MD$_{11}$ endosomal escape. We recently provided the first proof of concept that it can be used as carrier of therapeutic active molecules both in mammalian cells (Marchione *et al.* 2015) and in yeast cells (Marchione *et al.* 2014), demonstrating its promising potential for the development of new therapeutic strategies.

Competing interests

The authors declare that they have no competing interests.

References

Akashi K, Miyata H, Itoh H & Kinosita K Jr. 1996 Preparation of giant liposomes in physiological conditions and their characterization under an optical microscope. *Biophys J* **71** 3242-3250

Derossi D, Joliot AH, Chassaing G & Prochiantz A 1994 The third helix of the Antennapedia homeodomain translocates through biological membranes. *J Biol Chem* **269** 10444-10450

Deshayes S, Gerbal-Chaloin S, Morris MC, Aldrian-Herrada G, Charnet P, Divita G & Heitz F 2004 On the mechanism of non-endosomial peptide-mediated cellular delivery of nucleic acids. *BBA* **1667** 141-147

Eiriksdottir E, Mager I, Lehto T, El Andaloussi SH & Langel U 2010 Cellular internalization kinetics of (luciferin-)cell-penetrating peptide conjugates. *Bioconjugate Chem* **21** 1662-1672

Elliott G & O'Hare P 1997 Intercellular trafficking and protein delivery by a herpesvirus structural protein. *Cell* **88** 223-233

Elmquist A, Lindgren M, Bartfai T & Langel U 2001 VE-cadherin-derived cell-penetrating peptide, pVEC, with carrier functions. *Exp Cell Res* **269** 237-244

Frankel AD & Pabo CO 1988 Cellular uptake of the tat protein from human immunodeficiency virus. *Cell* **55** 1189-1193

Green M & Loewenstein PM 1988 Autonomous functional domains of chemically synthesized human immunodeficiency virus tat trans-activator protein. *Cell* **55** 1179-1188

Heitz F, Morris MC & Divita G 2009 Twenty years of cell-penetrating peptides: from molecular mechanisms to therapeutics *Br J Clin Pharmacol* **157** 195-206

Henriques ST & Castanho MA 2004 Consequences of nonlytic membrane perturbation to the translocation of the cell penetrating peptide pep-1 in lipidic vesicles. *Biochem* **43** 9716-9724

Hirose H, Takeuchi T, Osakada H, Pujals S, Katayama S, Nakase I, Kobayashi S, Haraguchi T & Futaki S 2012 Transient focal membrane deformation induced by arginine-rich peptides leads to their direct penetration into cells. *Mol Ther* **20** 984-993

Hoyer J, Schatzschneider U, Schulz-Siegmund M & Neundorf I 2012 Dimerization of a cell-penetrating peptide leads to enhanced cellular uptake and drug de-

livery. *Beilstein J Org Chem* **8** 1788-1797

Kyte J & Doolittle RF 1982 A simple method for displaying the hydropathic character of a protein. *J Mol Biol* **157** 105-132

Langel U 2006, in: E.L.U. CRC Press/Taylor & Francis (Ed.) Handbook of Cell-Penetrating Peptides, Boca Raton, London, New York.

Lundin P, Johansson H, Guterstam P, Holm T, Hansen M, Langel U & El Andaloussi SH 2008 Distinct uptake routes of cell-penetrating peptide conjugates. *Bioconjugate Chem* **19** 2535-2542

Madani F, Lindberg S, Langel U, Futaki S & Graslund A 2011 Mechanisms of cellular uptake of cell-penetrating peptides. *J Biophys* **2011** 414729

Marchione R, Daydé D, Lenormand JL & Cornet M 2014 ZEBRA cell-penetrating peptide as an efficient delivery system in Candida albicans. *Biotechnol J* **9** 1088-1094

Marchione R, Laurin D, Liguori L, Leibovitch MP, Leibovitch SA & Lenormand JL 2015 MD11-mediated delivery of recombinant eIF3f induces melanoma and colorectal carcinoma cell death. *Mol Ther Methods Clin Dev* **2** 14056

Milech N, Longville BA, Cunningham PT, Scobie MN, Bogdawa HM, Winslow S, Anastasas M, Connor T, Ong F, Stone SR, Kerfoot M, Heinrich T, Kroeger KM, Tan YF, Hoffmann K, Thomas WR, Watt PM & Hopkins RM 2015 GFP-complementation assay to detect functional CPP and protein delivery into living cells. *Sci Rep* **16** 18329

Mitchell DJ, Kim DT, Steinman L, Fathman CG & Rothbard JB 2000 Polyarginine enters cells more efficiently than other polycationic homopolymers. *J Pept Res* **56** 318-325

Palm-Apergi C, Lonn P & Dowdy SF 2012 Do cell-penetrating peptides actually "penetrate" cellular membranes? *Mol Ther* **20** 695-697

Park HH, Sohn Y, Yeo JW, Park JH, Lee HJ, Ryu J, Rhee WJ & Park TH 2014 Dimerization of 30Kc19 protein in the presence of amphiphilic moiety and importance of Cys-57 during cell penetration. *Biotechnol J* **9** 1582-1593

Petosa C, Morand P, Baudin F, Moulin M, Artero JB & Muller CW 2006 Structural basis of lytic cycle activation by the Epstein-Barr virus ZEBRA protein. *Mol Cell* **21** 565-572

Pooga M, Hallbrink M, Zorko M & Langel U 1998 Cell penetration by transportan. *FASEB J* **12** 67-77

Rothe R & Lenormand JL 2008 Expression and purification of ZEBRA fusion proteins and applications for the delivery of macromolecules into mammalian cells. *Curr Protoc Protein Sci* **18** 18.11

Rothe R, Liguori L, Villegas-Mendez A, Marques B, Grunwald D, Drouet E & Lenormand JL 2010 Characterization of the cell-penetrating properties of the Epstein-Barr virus ZEBRA trans-activator. *J Biol Chem* **285** 20224-20233

Säälik P, Elmquist A, Hansen M, Padari K, Saar K, Viht K, Langel U & Pooga M 2004 Protein cargo delivery properties of cell-penetrating peptides. A comparative study. *Bioconjugate Chem* **15** 1246-1253

Säälik P, Niinep A, Pae J, Hansen M, Lubenets D, Langel Ü & Pooga M 2011 Penetration without cells: membrane translocation of cell-penetrating peptides in the model giant plasma membrane vesicles. *J Control Release* **153** 117-125

Simons K & Ikonen E 1997 Functional rafts in cell membranes. *Nature* **387** 569-572

Terrone D, Sang SL, Roudaia L & Silvius JR 2003 Penetratin and related cell-penetrating cationic peptides can translocate across lipid bilayers in the presence of a transbilayer potential. *Biochem* **42** 13787-13799

Ziegler A 2008 Thermodynamic studies and binding mechanisms of cell-penetrating peptides with lipids and glycosaminoglycans. *Adv Drug Deliv Rev* **60** 580-597

Zorko M & Langel U 2005 Cell-penetrating peptides: mechanism and kinetics of cargo delivery. *Adv Drug Deliv Rev* **57** 529-545